International Journal of Mass Spectrometry 274 (2008) 21–24

Contents lists available at ScienceDirect

International Journal of Mass Spectrometry

journal homepage: www.elsevier.com/locate/ijms

Matrix-assisted laser desorption ionization of infrared laser ablated particles

Fan Huang, Xing Fan, Kermit K. Murray*

Department of Chemistry, Louisiana State University, Baton Rouge, Louisiana 70803, United States

ARTICLE INFO

Article history:
Received 18 December 2007
Received in revised form 20 March 2008
Accepted 10 April 2008
Available online 18 April 2008

Keywords:
Infrared
MALDI
Laser
Ablation

ABSTRACT

An infrared (IR) laser was used to ablate particles that were subsequently ionized by matrix-assisted laser desorption ionization (MALDI). Infrared light from a pulsed optical parametric oscillator (OPO) laser system was directed at a solid sample under vacuum containing a 2,5-dihydroxybenzoic acid (DHB) matrix and peptide or protein analyte. A pulsed 351 nm ultraviolet (UV) excimer laser that was directed 1.4 mm above and parallel to the sample surface was used to irradiate the ablated material in the desorption plume. Ions created by post-ablation ionization were detected with a linear time-of-flight (TOF) mass spectrometer. Mass spectra of the peptide bradykinin and proteins bovine insulin and cytochrome *c*, were recorded. Under these conditions, two simultaneous mass spectra were generated: an IR–MALDI mass spectrum from the OPO and a UV post-ablation spectrum generated by irradiating material in the plume. Factors affecting the two-laser ion yield were studied, including the delay time between the laser pulses and the fluence of the IR and UV laser.

1. Introduction

Matrix-assisted laser desorption ionization (MALDI) mass spectrometry (MS) has become a standard technique for the study of large biological and synthetic macromolecules [1]. MALDI is typically performed with a single laser operating in the ultraviolet (UV) wavelength range between 260 and 360 nm, and matrices absorbing in this wavelength range are used in almost all UV MALDI studies [2]. Alternatively, MALDI has also been performed using lasers operating in the infrared (IR) wavelength range [3,4]. Although IR and UV lasers produce comparable MALDI mass spectra, the propensity for IR lasers to remove large quantities of material makes this approach more difficult to use for routine analysis [5,6]. However, the ability to use intrinsic solvents as the matrix and the relatively soft ionization of large biomolecules make it attractive in certain cases. IR lasers have also been used with success for atmospheric pressure MALDI and IR laser assisted desorption electrospray ionization [7,8].

IR lasers can be used in combination with UV lasers to combine the material heating and removal ability of the former with the ionization efficiency of the latter. The two lasers can be directed at the same spot on the sample target and the energy adjusted so that ions are produced only when both lasers are fired [9]. The time delay between the two pulses is adjusted to maximize the ion signal. An IR laser directed at the sample target heats and, in some cases, melts the sample material, which results in more efficient UV laser ionization. Another two-laser approach uses the IR laser to desorb and ablate material, and the second laser to irradiate the plume of material. With this approach the desorption and ionization processes are separated, allowing them to be optimized independently in some cases. Using this approach, many low mass (typically a few thousand Da) compounds can be post-ionized with good signal intensity [10].

Large molecules can be ionized from suspended particulate material that has been sprayed or ablated. For example, particles sprayed from a solution containing matrix and analyte [11] or coated with matrix by condensation [12] will produce ions from relatively large biomolecules when irradiated with a UV laser. A similar result was obtained when an IR laser was used to desorb and ablate material from a solid sample and a second IR laser was used for ionization [13]. Ions from large biomolecules were observed that are not expected from multiphoton ionization of free molecules. It is known that IR lasers ablate large quantities of particulate [14], suggesting that laser desorption ionization of the ablated particulate is a key component of the ionization process. Desorption of material into a continuous electrospray has also been performed using IR lasers to ablate the analyte as particulate [7,8]. An improved understanding of the processes involved in the ablation of particulate and subsequent ionization has the potential to lead to better IR laser ablation and ionization in mass spectrometry.

In this article, we report IR laser ablation with UV laser irradiation of the desorbed and ablated plume of material. A tunable pulsed IR optical parametric oscillator (OPO) laser was used for sample ablation, and a 351 nm UV excimer laser was used for post-particle ablation and ionization. The matrix 2,5-dihydroxybenzoic

* Corresponding author.
E-mail address: kkmurray@lsu.edu (K.K. Murray).

1387-3806/$ – see front matter © 2008 Elsevier B.V. All rights reserved.
doi:10.1016/j.ijms.2008.04.006

acid (DHB) and peptide and protein molecular weight standards bradykinin, bovine insulin and cytochrome *c* were used to demonstrate the process. The relation between ion yield and such factors as delay time between the IR and UV lasers and IR and UV laser fluence was explored.

2. Experimental

2.1. Mass spectrometry

All experiments were carried out using a home-built linear time-of-flight mass spectrometer that has been described in detail previously [15]. Briefly, ions that were generated by the IR laser or the IR and UV laser in combination were accelerated to 18 kV using a single stage of acceleration with an 18 mm gap. The ions were mass separated in a field free region of a 1 m flight tube with a 25 mm microchannel plate detector. Data were recorded with a 500 MHz digital oscilloscope (9350CM; Lecroy, Chestnut Ridge, NY, USA) that was triggered by a pulse delay generator (DG535; Stanford Research Systems, Sunnyvale, CA, USA) that also controlled the laser timing. Mass spectra were averaged on the oscilloscope and transferred to a computer or, for ion yield measurements, peak areas were integrated on the oscilloscope and the results were transferred to the computer.

2.2. Two-laser arrangement

The IR laser system was a wavelength tunable OPO (Mirage 3000B, Continuum, Santa Clara, CA) that was run at a 2 Hz repetition rate. In this study, the data were acquired at an IR wavelength of either 2.94 or 3.05 μm. The IR beam was attenuated using a combination of optical flats and focused using a 250 mm spherical lens onto the sample surface at an angle of 45°. The spot size was 200 μm × 280 μm, measured using laser burn paper. The IR laser pulse width is 5 ns. The UV laser was 351 nm excimer laser (Optex, Lambda Physik, Ft. Lauderdale, FL) that was synced with the IR laser. The UV laser was attenuated using a variable number of glass microscope slides. The UV beam was directed above and parallel to the sample surface with a distance of 1.4 mm between the center of the UV beam and the sample surface. Focusing of the UV beam was achieved using a 254 mm focal length fused-silica lens and the spot size was 500 μm × 1000 μm with the long axis parallel to the target surface. The pulse width of the UV laser is 8 ns. The laser energy for both lasers was measured using a pyroelectric joule meter (Model ED-104AX, Gentec, Inc., Palo Alto, CA).

2.3. Data acquisition

Each mass spectrum shown below was an average of 20 single laser shots. For the UV ionization ion yield studies, Δt refers to the time difference between IR and UV laser pulses, and was set by the pulse delay generator. The data acquisition sequence has been described previously [16]. The pulse generator and oscilloscope were both controlled by the data acquisition computer that set the delay between the IR and UV laser pulses at the pulse generator. The integrated peak area for the selected time range was then read from the oscilloscope and recorded on the computer. The delay time was incremented and the peak integration process was repeated at the new Δt. After one sweep through the full range of Δt values, the pulse generator was reset to the starting Δt and the data acquisition process was repeated. The sequence of data acquisition over the full range of delay time values was repeated five times to generate each plot and each data point resulted from an average of 20 laser shots. The sample target was rotated at one revolution every 2 min using a variable speed motor to provide a fresh sample spot for each laser shot. For the study of ion yield as a function of fluence, the peak area values were recorded from the oscilloscope without being transferred to the computer. The laser energy measurements were repeated five times and the average laser energy was combined with laser spot size to obtain the fluence.

2.4. Sample preparation

The following reagents were obtained from Sigma (St. Louis, MO, USA) and used without further purification: bradykinin (B3259), cytochrome *c* from bovine heart (C3131), bovine insulin (I5500) and 2,5-dihydroxy benzoic acid (G5254). Analyte and matrix solutions were prepared in 970 μl methanol with 30 μl 1% trifluoroacetic acid (TFA; Fisher, Fair Lawn, NJ, USA) in distilled water (house supply). The concentration for each solution was 0.5 mM for bradykinin, 0.52 mM for insulin, 0.42 mM for cytochrome *c* and 0.44 M for DHB. The analyte to matrix molar ratio of each matrix and analyte solution mixture was 1:1500 for bradykinin, 1:1000 for insulin and 1:2000 for cytochrome *c*. After the solution was mixed well, 24 μl mixture was deposited on a stainless steel sample target with a diameter of 8 mm for a typical dried droplet spot.

3. Results and discussion

Mass spectra of the peptide bradykinin with a DHB matrix using IR and both IR and UV lasers are shown in Fig. 1. Fig. 1a was obtained using only the IR laser at 2.94 μm with a fluence of 5.2 kJ/m^2; the zero of the *x*-axis corresponds to the firing of the IR laser. The peaks with flight times less that 10 μs correspond to matrix ions and associated adducts with masses less than 300 Da. The protonated bradykinin molecule $[M+H]^+$, that results from IR laser desorption ionization is observed at a flight time of 19.7 μs. No signal was obtained at a UV laser fluence of 1.4 kJ/m^2 (not shown). Fig. 1b was obtained using both IR and UV lasers at a delay time of 50 μs with IR and UV laser fluences of 5.2 and 1.4 kJ/m^2, respectively. Under these conditions, a mass spectrum similar to that observed in Fig. 1a is observed in the time region below 20 μs, but new features are observed between 50 and 80 μs. The additional peaks

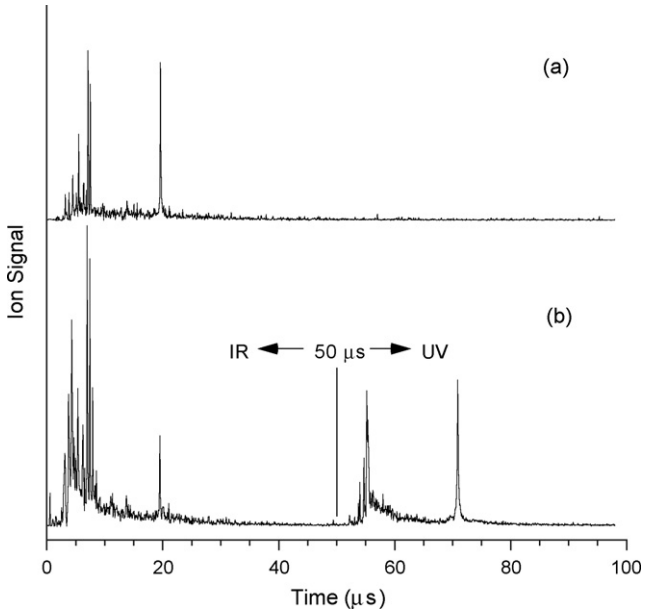

Fig. 1. Bradykinin mass spectra with different laser conditions: (a) 2.94 μm IR laser only and (b) IR and UV lasers at Δt = 50 μs; no signal was obtained with the 351 nm laser only.

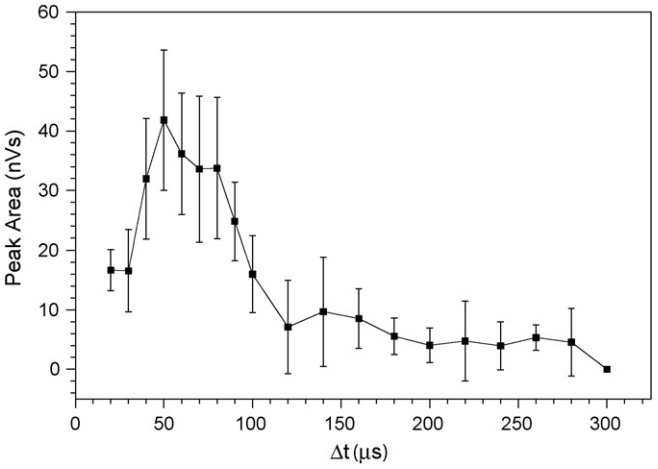

Fig. 2. Signal intensity of singly charged molecular bradykinin ions as a function of delay time.

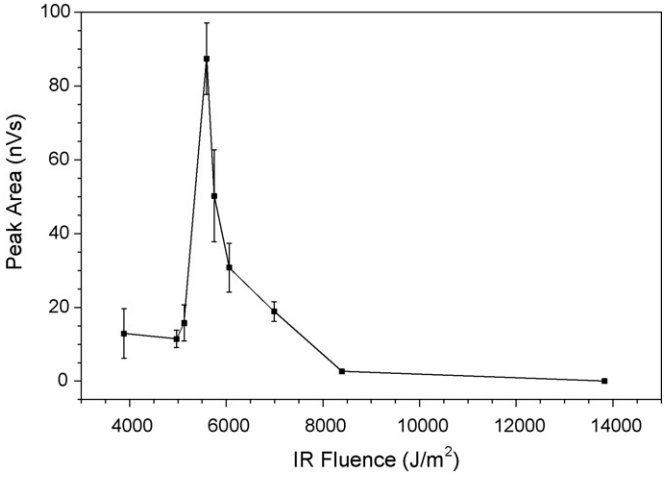

Fig. 3. Signal intensity of singly charged molecular bradykinin ions as a function of IR laser fluence.

resemble those resulting from the IR laser radiation, but are displaced by the 50 μs time delay. The cluster of peaks between 52 and 60 μs are displaced by about 50 μs from the IR laser generated matrix peaks and the peak at 71 μs is displaced by 51.3 μs from the IR laser generated bradykinin peak. This latter peak is assigned as protonated bradykinin that was ablated from the target by the IR laser and ionized by the UV laser. The longer flight time for the bradykinin produced with the UV laser is due to the fact that the ions are formed above the target surface and are therefore accelerated through a lower potential difference. It was in all cases nearly impossible to suppress the IR MALDI signal because the IR laser energy required for the two-laser signal was in most cases sufficient for the production of ions. It should also be noted that no two-laser analyte signal could be obtained using a glycerol IR matrix although low mass ions could be observed.

Fig. 2 shows the delay time dependence of the intensity of the two-laser protonated bradykinin peak under conditions similar to those used to obtain Fig. 1b. The IR fluence was 5.6 kJ/m^2, the UV fluence was 1.4 kJ/m^2 and delay time ranged from 20 to 300 μs. Although signal from protonated bradykinin could be obtained with delay times as low as 12 μs, interferences from the IR laser mass spectrum prevented accurate measurements of the peak area below 20 μs. The peak area rises as delay time increases from 20 to 50 μs and the signal reaches a maximum near 50 μs. The signal drops rapidly between 50 and 120 μs and then more slowly after that to 300 μs. After 300 μs, signal could be observed, but it was weak and not reproducible.

Fig. 3 displays a plot of the two-laser bradykinin $[M+H]^+$ peak area, plotted as a function of the IR laser fluence. The delay time was 50 μs and the UV laser fluence was 1.4 kJ/m^2. This figure indicates that, in order to achieve optimum signal intensity, the IR laser energy must be in a relatively narrow range between 5 and 7 kJ/m^2. Under these conditions, the maximum two-laser signal occurred at an IR fluence of 5.6 kJ/m^2.

The bradykinin two-laser $[M+H]^+$ peak area plotted as a function of the UV laser fluence is shown in Fig. 4. The delay time was 50 μs and the IR laser fluence was 5.6 kJ/m^2. The UV laser fluence dependence shows a gradual rise starting at the threshold of 0.8 kJ/m^2, below which no signal was observed. Above this threshold fluence, the peak area increases linearly with the UV fluence. In the range tested up to 2 kJ/m^2, the signal continued to rise with laser fluence, suggesting that a better signal intensity might be obtained if the UV fluence were increased to still higher levels. The need for high UV laser energies has been observed previously in aerosol MALDI [17].

Protein standards were investigated using the post-ablation ionization method. Fig. 5 displays two representative mass spectra of cytochrome *c* (Fig. 5a) and insulin (Fig. 5b) in a DHB matrix with IR wavelength at 3.05 μm. It was found that this wavelength, which corresponds to the IR absorption maximum of DHB [18], gave the best results for the two-laser protein mass spectra. The peaks at 139 μs in Fig. 5a and at 107 μs in Fig. 5b correspond to cytochrome *c* and insulin, respectively. For the cytochrome *c* mass spectrum, the delay time was 70 μs, and the IR and UV fluencies were 8.4 and 1.4 kJ/m^2, respectively. For the insulin mass spectrum, the delay time was 60 μs and the IR and UV fluences were 3.8 and 1.4 kJ/m^2, respectively. Although the maximum in the ion signal was obtained with an approximately 50 μs delay, an additional delay was added for the larger proteins to avoid overlap of the one and two-laser mass spectra. Factors affecting the protein mass spectra were not studied since the signal intensity under our experimental conditions was not high and it was therefore difficult to obtain reproducible results.

Two possibilities for ionization of biomolecules in the plume of desorbed and ablated material are the multiphoton ionization of free molecules and the ionization of particles containing matrix and analyte. The observation of biomolecules of the size of insulin and cytochrome *c* (Fig. 5) argues strongly against a multiphoton ionization mechanism. Molecules of this size are difficult to ionize

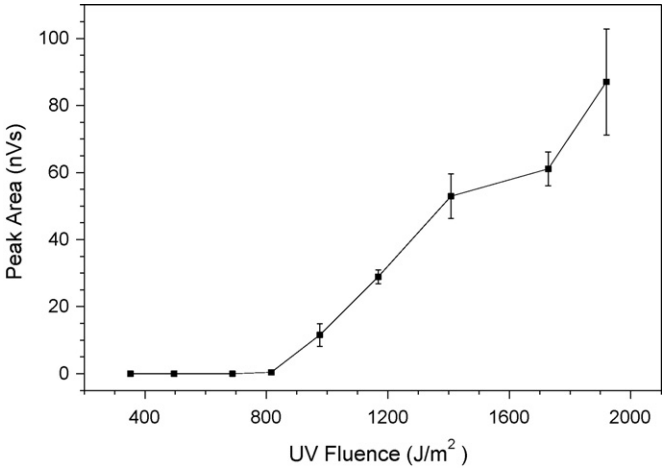

Fig. 4. Signal intensity of singly charged molecular bradykinin ions as a function of UV laser fluence.

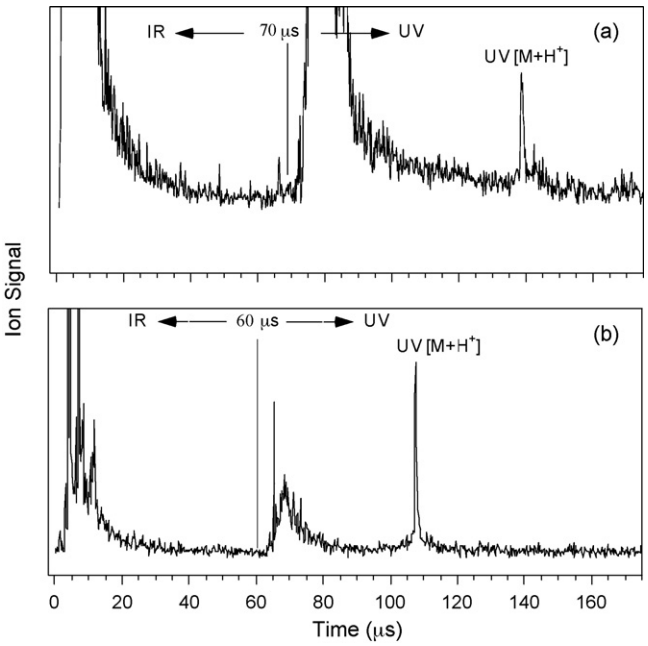

Fig. 5. IR/UV post ionization mass spectra of (a) cytochrome *c* at $\Delta t = 70\ \mu s$ and (b) insulin at $\Delta t = 60\ \mu s$.

through the absorption of multiple photons due to the efficient energy dissipation in the large number of vibrational degrees of freedom [10]. Instead, these results suggest that particles containing a UV MALDI matrix and analyte, when irradiated with the UV laser, form ions by a MALDI process. It has been observed that particles containing matrix and analyte, when sprayed into vacuum and irradiated with a UV laser, form ions by MALDI [11,17]. A particle MALDI mechanism has been suggested previously for IR laser ablated particles that were irradiated with a second IR laser. However, in this case, the absorption of the second IR laser energy by the analyte molecule [19] or waters of hydration [20] cannot be ruled out. The observation of ions from proteins by UV irradiation of the ablated material strongly suggests that the ionization mechanism is MALDI of the ablated particles. This hypothesis is supported by results of time-resolved fast-flash photography of the glycerol plume [21] and by measurements of the particle size and number ablated by an IR laser from a MALDI matrix [14], which show a large number of particles in the IR ablation plume.

The velocity of the IR laser desorbed material can be estimated using the appearance of two-laser signal as an indication for the arrival time of the plume front. For UV MALDI, the axial velocity is between 200 and 1000 m/s for ions, 600 and 800 m/s for neutrals [2]. The previous study of IR laser ablation and IR ionization found that the axial velocity of the plume front corresponding to the initial rise in ion signal represented a plume front velocity of 1000 m/s [13]. In our work, the velocity of the plume expansion can be calculated by dividing the distance between the UV beam center and the sample surface (1.4 mm) by the delay time for observation of UV ions (50 μs for the maximum ion yield in Fig. 2). The calculated velocity is about 30 m/s, which is more than an order of magnitude slower than expected. However, it is also possible that material is ejected after the end of the laser pulse, which would lead to an anomalously low estimate to the ejection velocity [22]. Such delayed emission of IR ablated particulate has been observed using fast photography [23], photoacoustic [24], and time-resolved particle size measurements [22]. It is possible that the UV laser is less efficient at ionizing biomolecules in the early part of the plume compared to the IR laser used in the previous study. This would lead to the delayed signal onset and the low apparent particle velocity observed in this study.

4. Conclusions

An infrared ablation/post-ultraviolet matrix-assisted laser desorption ionization method is presented. Using this method, mass spectra of biomolecules including bradykinin, insulin, and cytochrome *c* were obtained with a 2,5-dihydroxybenzoic acid matrix but could not be obtained using the IR matrix glycerol. Two-laser signal could be obtained at IR laser fluences between 5 and 8 kJ/cm^2. The signal increased with UV laser fluence and was the optimum at the maximum of 2 kJ/cm^2. The observation of signal from proteins larger than 10 kDa suggests that ionization proceeds through the ablation particles containing a mixture of matrix and analyte followed by UV MALDI of these particles.

Acknowledgement

This work was supported by the National Science Foundation, Grant Number CHE-0415360.

References

[1] F. Hillenkamp, J. Peter-Katalinic, MALDI MS—A Practical Guide to Instrumentation Methods and Applications, Wiley–VCH, Weinheim, 2007.
[2] K. Dreisewerd, Chem. Rev. 103 (2003) 395.
[3] K. Dreisewerd, S. Berkenkamp, A. Leisner, A. Rohlfing, C. Menzel, Int. J. Mass Spectrom. 226 (2003) 189.
[4] K.K. Murray, in: R.M. Caprioli, M.L. Gross (Eds.), Encyclopedia of Mass Spectrometry, Elsevier, 2006.
[5] R. Cramer, A.L. Burlingame, Rapid Commun. Mass Spectrom. 14 (2000) 53.
[6] D.J. Rousell, S.M. Dutta, M.W. Little, K.K. Murray, J. Mass Spectrom. 39 (2004) 1182.
[7] P. Nemes, A. Vertes, Anal. Chem. 79 (2007) 8098.
[8] Y.H. Rezenom, J. Dong, K.K. Murray, Analyst 133 (2008) 226.
[9] X. Tang, M. Sadeghi, Z. Olumee, A. Vertes, Rapid Commun. Mass Spectrom. 11 (1997) 484.
[10] J. Grotemeyer, E.W. Schlag, Acc. Chem. Res. 22 (1989) 399.
[11] K.K. Murray, D.H. Russell, J. Am. Soc. Mass Spectrom. 5 (1994) 1.
[12] P.G. Carson, K.R. Neubauer, M.V. Johnston, A.S. Wexler, J. Aero. Sci. 26 (1995) 535.
[13] A. Leisner, A. Rohlfing, S. Berkenkamp, F. Hillenkamp, K. Dreisewerd, J. Am. Soc. Mass Spectrom. 15 (2004) 934.
[14] S.N. Jackson, J.-K. Kim, J.L. Laboy, K.K. Murray, Rapid Commun. Mass Spectrom. 20 (2006) 1299.
[15] M.W. Little, K.K. Murray, Int. J. Mass Spectrom. 261 (2007) 140.
[16] M.W. Little, J.K. Kim, K.K. Murray, J. Mass Spectrom. 38 (2003) 772.
[17] L. He, K.K. Murray, J. Mass Spectrom. 34 (1999) 909.
[18] M. Sinha, SPIE (1991) 150.
[19] M.W. Little, J. Laboy, K.K. Murray, J. Phys. Chem. C 111 (2007) 1412.
[20] S. Berkenkamp, M. Karas, F. Hillenkamp, Proc. Natl. Acad. Sci. USA 93 (1996) 7003.
[21] A. Leisner, A. Rohlfing, U. Rohling, K. Dreisewerd, F. Hillenkamp, J. Phys. Chem. B 109 (2005) 11661.
[22] X. Fan, K.K. Murray, Appl. Surf. Sci., in press.
[23] I. Apitz, A. Vogel, Appl. Phys. A: Mater. Sci. Process. 81 (2005) 329.
[24] A. Rohlfing, C. Menzel, L.M. Kukreja, F. Hillenkamp, K. Dreisewerd, J. Phys. Chem. B 107 (2003) 12275.